Supplementary Information

Amorphous Ta_2O_5 memristor with excellent self-selective and artificial synaptic properties for artificial neural networks

Bumjoo Kim[a], Geun-Soo Lee[a], San Kwak[a], Byeong-Jae Min[a], Boo-Hyun Choi[a], Hyun-Ju Choi[a], Jichai Jeong[b] and Sahn Nahm[a,].*

[a] Department of Materials Science and Engineering, Korea University, 145 Anam-ro Seongbuk-gu, Seoul 02841, Republic of Korea

[b] Department of Brain and Cognitive Engineering, Korea University, 145 Anam-ro Seongbuk-gu, Seoul 02841, South Korea

[*]Corresponding author Email *address:* snahm@korea.ac.kr

1. *I-V* curves of ATO films grown under various atmospheres

Figs. S1(a)-(d) provide the *I-V* curves of the ATO films grown under various Ar and O_2 atmospheres without the RTA under O_2 atmosphere. The ATO film grown under an Ar and O_2 atmosphere at a ratio of 1:1 shows a typical bipolar switching *I-V* plot with a set voltage of –1.9 V and a reset voltage of 1.6 V (Fig. S1(a)). The switching properties of this ATO memristor can be explained by the formation and destruction of oxygen vacancy filaments. This ATO film always showed a typical bipolar switching *I-V* plot; thus, this film cannot be used as a tunneling barrier for the induction of self-selective characteristics. Similar results were also obtained from the other ATO films, as shown in Figs. S1(b)-(d). Hence, they cannot be used as the tunneling barrier for self-selectivity. Fig. S1(e) shows the *I-V* curve of the film grown under Ar and O_2 atmosphere at a ratio of 3:1, with the RTA process conducted under an O_2 atmosphere. This film also showed a bipolar switching curve without insulating properties because it was grown in an oxygen-deficient atmosphere ($Ar:O_2$ = 3:1), resulting in the formation of numerous oxygen vacancies in the film. However, when the film was grown under an Ar and O_2 atmosphere at a ratio of 1:1 with subsequent RTA under an O_2 atmosphere, insulating properties were observed, as shown in Fig. 2(c). Therefore, it can be suggested that the performance of IATO film is greatly affected by the amount of oxygen vacancies in film that can be controlled by the atmosphere during growth and RTA processes.

The chemical uniformity of the IATO film was examined using EDX analysis, as shown in Fig. S1(f). The ratio of Ta^{+5} and O^{-2} ions is ~ 2.45, which is close to the theoretical value of 2.5, indicating that the IATO film grown by RF sputter has a chemically uniform surface. Therefore, the IATO films grown in the TiN substrate usually have physically and chemically uniform surface.

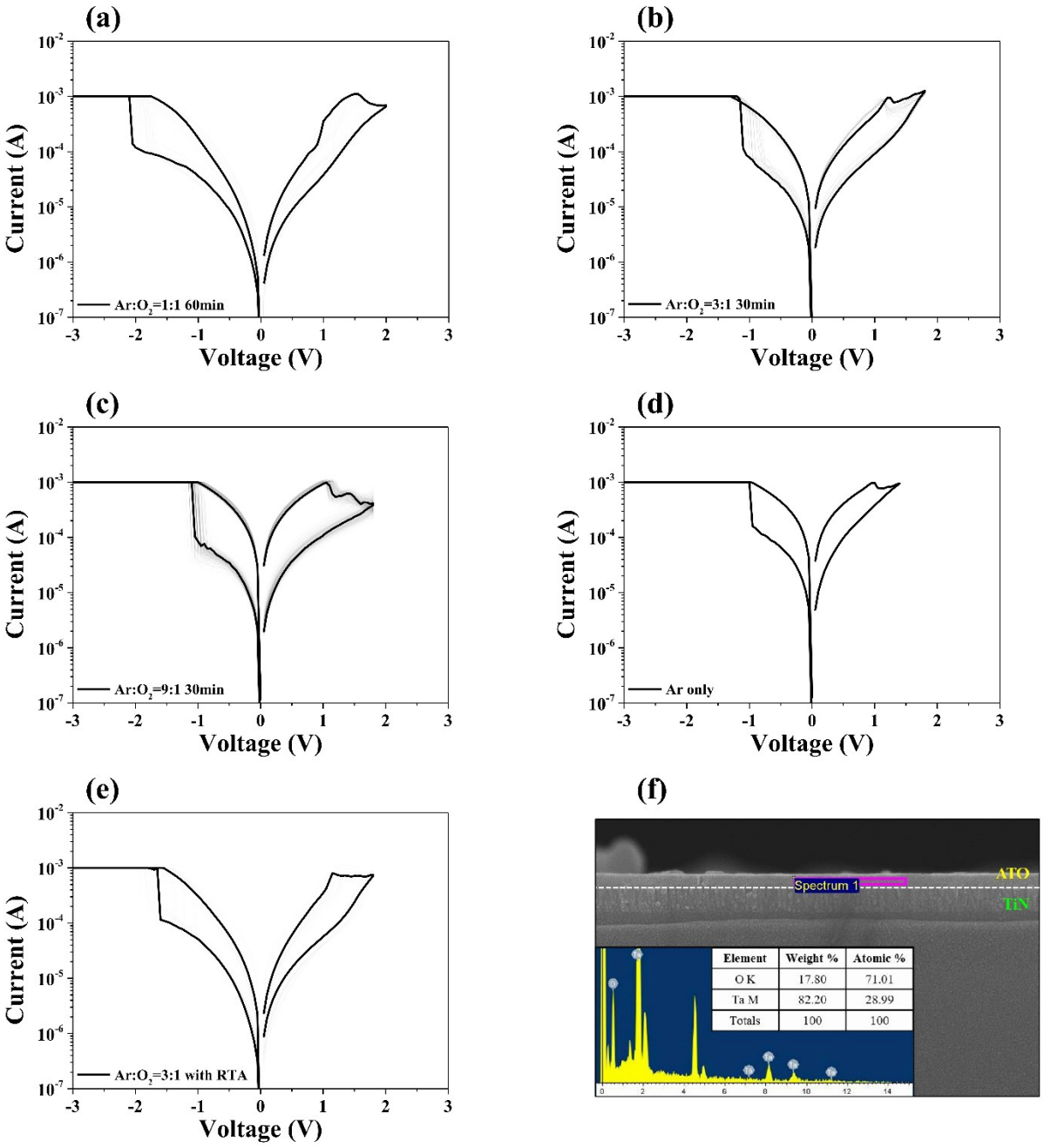

Figure S1. *I-V* curves of the ATO films grown under various Ar and O_2 atmospheres without the RTA process; (a) Ar:O_2 = 1:1, (b) Ar:O_2 = 3:1, (c) Ar:O_2 = 9:1 and (d) Ar-only atmosphere. (e) *I-V* curve of the ATO film grown under the Ar and O_2 atmosphere at a ratio of 3:1 with the RTA process conducted under an O_2 atmosphere. (f) EDX spectrum of the IATO film grown on the TS substrate.

2. Breakdown voltage of the IATO film deposited under various RTA times

Fig. S2 shows the *I-E* curves of the 30-nm-thick ATO films annealed at various RTA times, which provide the breakdown electric field of the ATO films. The ATO film formed without the RTA process under the O_2 atmosphere showed a relatively small breakdown electric field of 0.14 V/nm owing to numerous oxygen vacancies. The breakdown electric field increased with RTA time (Fig. S2), probably because of the decrease in the number of oxygen vacancies. The ATO film grown under the RTA time of 20 min revealed the maximum electric field of 0.22 V/nm; this ATO film can be used for the tunneling barrier to induce the self-selective properties in the ATO memristor. However, when the RTA time exceeded 20 min, the breakdown electric field decreased because of the formation of interstitial oxygen ions, which increased the conductivity of the ATO film. Therefore, the appropriate RTA time to produce an IATO thin film depends on the thickness of the ATO film.

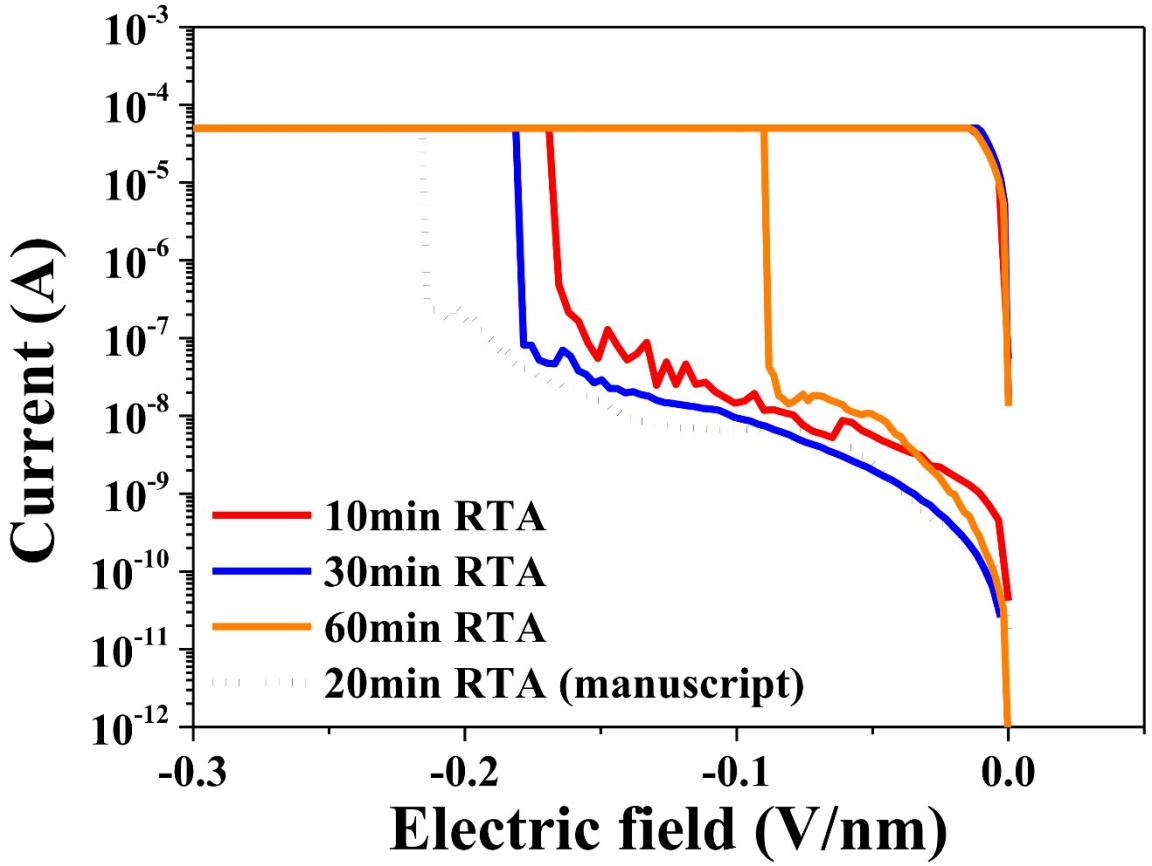

Figure S2. *I-V* curve of the 30-nm-thick ATO films annealed under various RTA times.

3. *I-V* curves of the ATO/IATO devices with various IATO thicknesses

Figs. S3(a)-(c) show the *I-V* curves of ATO/IATO devices with various IATO thicknesses. When the thickness of the IATO film is less than approximately 5.5 nm, it cannot behave as an insulating layer (or tunneling barrier); thus, the ATO/IATO device provides typical bipolar switching properties without self-selective properties (Figs. S3(a) and (b)). However, when the IATO film thickness reached approximately 7.3 nm, the ATO/IATO device behaved as an insulator (Fig. S3(c)). The ATO/IATO device exhibits selective properties when the thickness of the IATO film is close to 5.5 nm, as provided in Fig. 3(c), indicating that the thickness of IATO film is very important to obtain self-selective behavior.

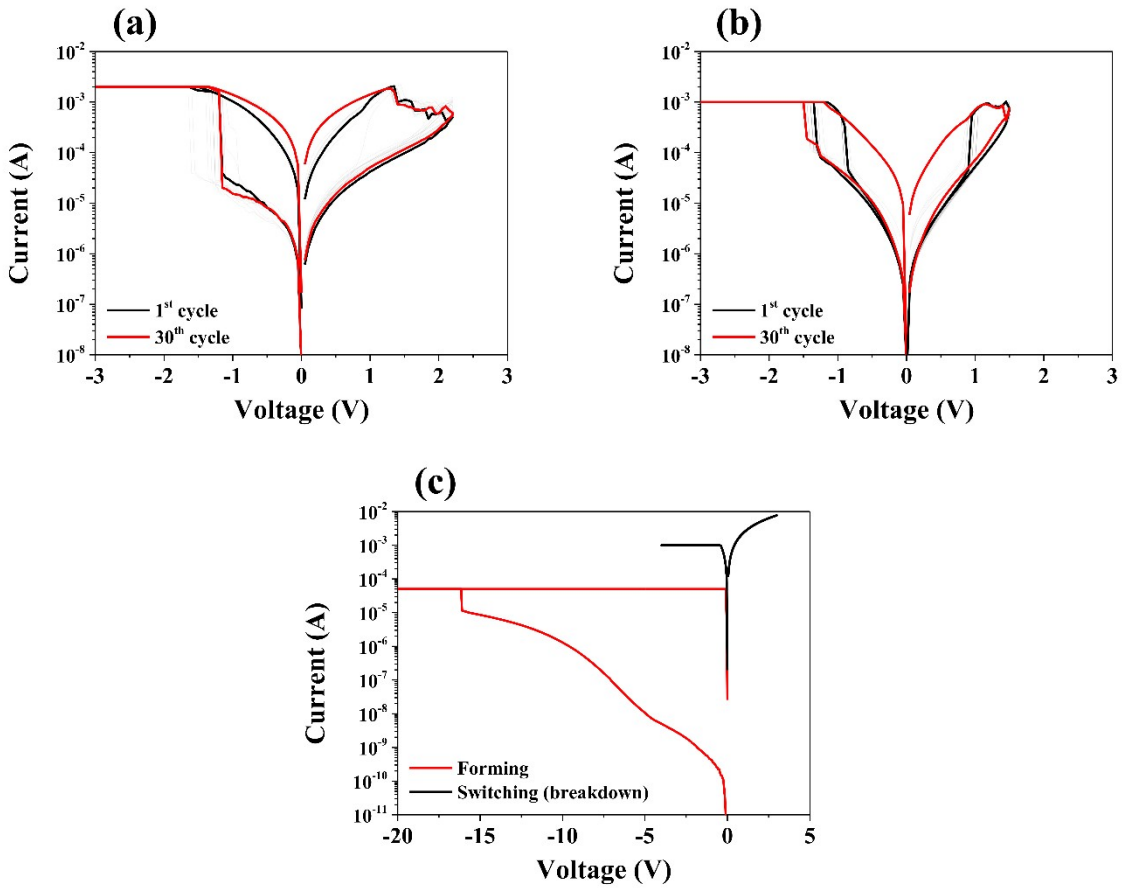

Figure S3. *I-V* curves of the ATO/IATO devices with various IATO layer thicknesses; (a) 1.8 nm, (b) 3.7 nm, and (c) 7.3 nm.

4. Various electrical properties of the ATO/IATO/TS memristor

Fig. S4(a) shows the I_{LRS}/I_{HRS} (or ON/OFF ratio) and nonlinearity of the Pt/ATO/IATO/TS memristor measured at a positive voltage. This memristor shows the maximum I_{LRS}/I_{HRS} of 23.3 and nonlinearity of 118.9 at 1.25 V, as indicated by the dotted line in Fig. S4(a). Identical results were also obtained at –1.3 V, as shown in Fig. 3(a). Therefore, the Pt/ATO/IATO/TS memristor exhibits good self-selective properties. The retention properties of Pt/ATO/IATO/TS memristors were also investigated (Fig. S4(b)), and the reading voltages of the currents in the LRS and HRS were 0.65 V. The currents in the LRS and HRS were well-preserved for up to 10^3 s (Fig. S4(b)). Moreover, the currents in the LRS and HRS were preserved after 10^3 s at a reading voltage of 1.25 V (Fig. 3(e)). Therefore, the Pt/ATO/IATO/TS memristor was considered to possess good retention properties. Fig. S4(c) shows the endurance characteristics of the Pt/ATO/IATO/TS memristor; the LRS and HRS currents were obtained at 0.65 V. The currents in the LRS and HRS did not change over 300 cycles (Fig. S4(c)), with identical results obtained at a reading voltage of 1.25 V, as shown in Fig. 3(f). Therefore, this memristor was considered to exhibit good retention characteristics. These results clearly show that the Pt/ATO/IATO/TS memristor has excellent self-selective properties and reliability.

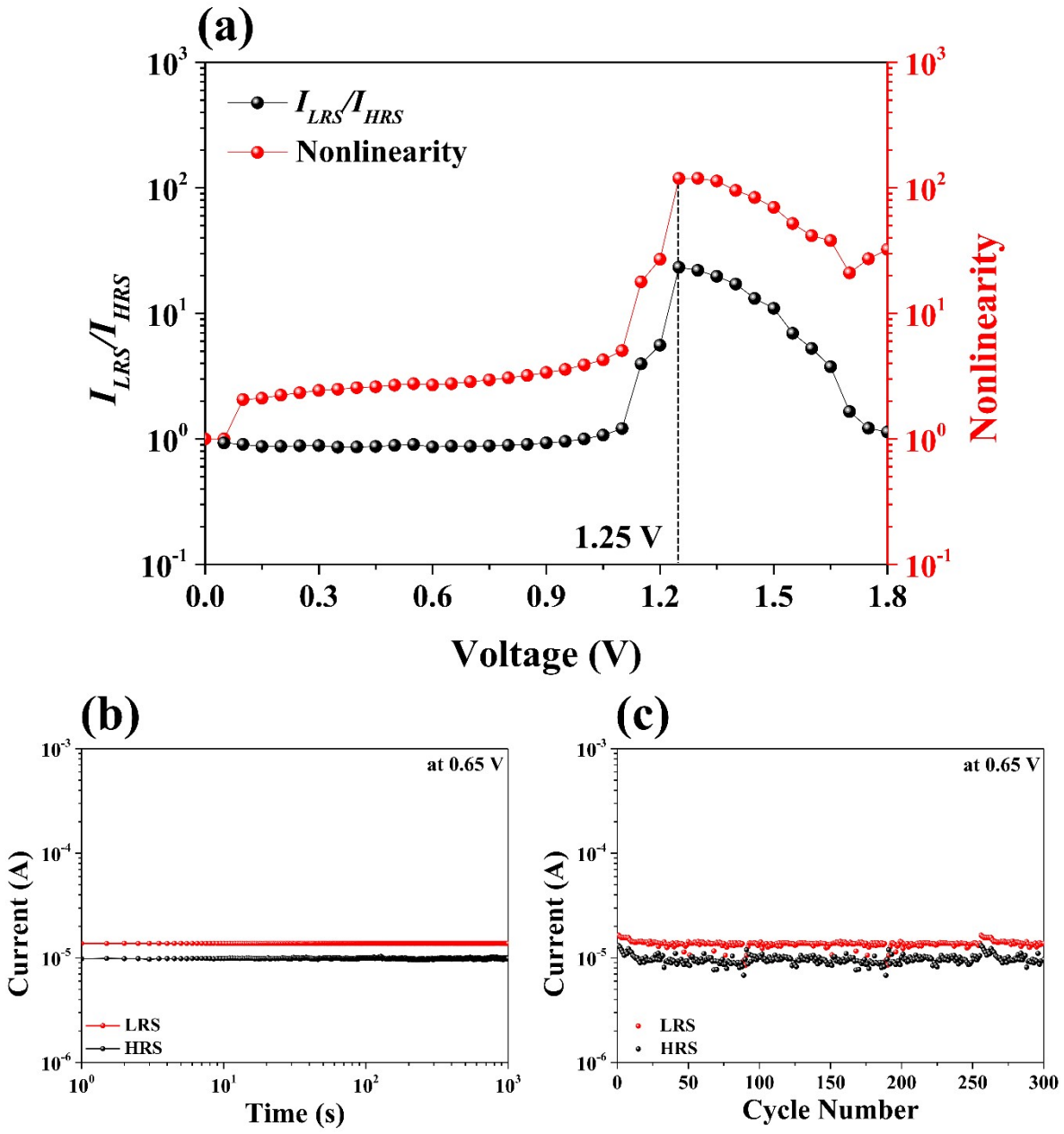

Figure S4. (a) I_{LRS}/I_{HRS} and the nonlinearity of the Pt/ATO/IATO/TS memristor. (b) Retention and (c) endurance properties of the ATO film deposited on the IATO/TS substrate.

5. O1s XPS spectra obtained from the ATO thin film

The O1s XPS spectra of the ATO thin film in the LRS and HRS are shown in Figs. S5(a) and (b), respectively. The O1s spectra show two peaks at 530 eV and 531.4 eV, corresponding to lattice and non-lattice oxygen, respectively[1]. The O1s spectra of the Pt/ATO/IATO/TS memristor in the LRS exhibited an intense peak corresponding to the non-lattice oxygen peak (Fig. S5(a)). Hence, oxygen vacancies are present in the ATO thin film. Therefore, many oxygen ions drift from the ATO film to the TiN electrode during the set process, producing numerous oxygen vacancies in the ATO film. In contrast, the O1s spectra of the ATO film of the Pt/ATO/IATO/TS memristor in the HRS showed a lattice oxygen peak but no peak corresponding to non-lattice oxygen (Fig. S5(b)), suggesting that the ATO thin film in the HRS contained a small number of oxygen vacancies. Therefore, the results obtained from the O1s XPS spectra are similar to those obtained from the N1s XPS spectra (Figs. 4(c) and (d)).

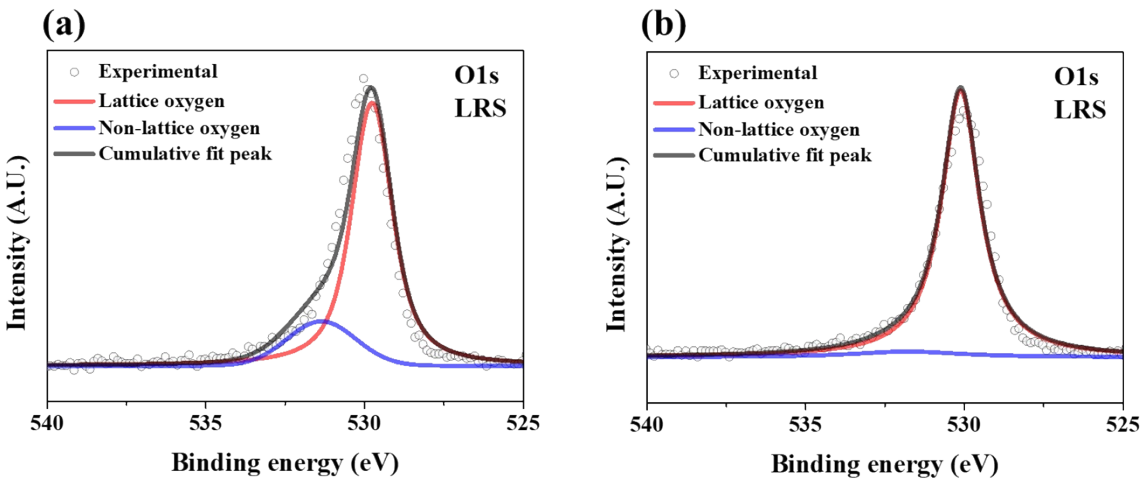

Figure S5. O1s XPS spectra obtained from the ATO thin film in (a) LRS and (b) HRS.

6. Two types of tunneling mechanisms

There are two types of tunneling mechanisms: direct tunneling (DT) and Fowler–Nordheim tunneling (FNT)[2,3]. An applied voltage smaller than the barrier height (ø) causes DT, as shown in Fig. S6(a). In contrast, an applied voltage greater than the barrier height causes FNT, as shown in Fig. S6(b). The relationship between the tunneling current and applied voltage can be expressed as follows[2,3]:

$$I \propto \begin{cases} V exp\left(-\frac{2d\sqrt{2m^{*}\emptyset}}{\hbar}\right) & \left(V < V_{trans}\right) : DT \qquad (S1) \\ V^{2}\exp\left(-\frac{4d\sqrt{2m^{*}\phi^{3}}}{3\hbar eV}\right) & \left(V > V_{trans}\right) : FNT \qquad (S2) \end{cases}$$

Moreover, Eqs. (S1) and (S2) can be rewritten in terms of $\ln(I/V^2)$ and $(1/V)$, respectively, as expressed in Eqs. (1) and (2), respectively:

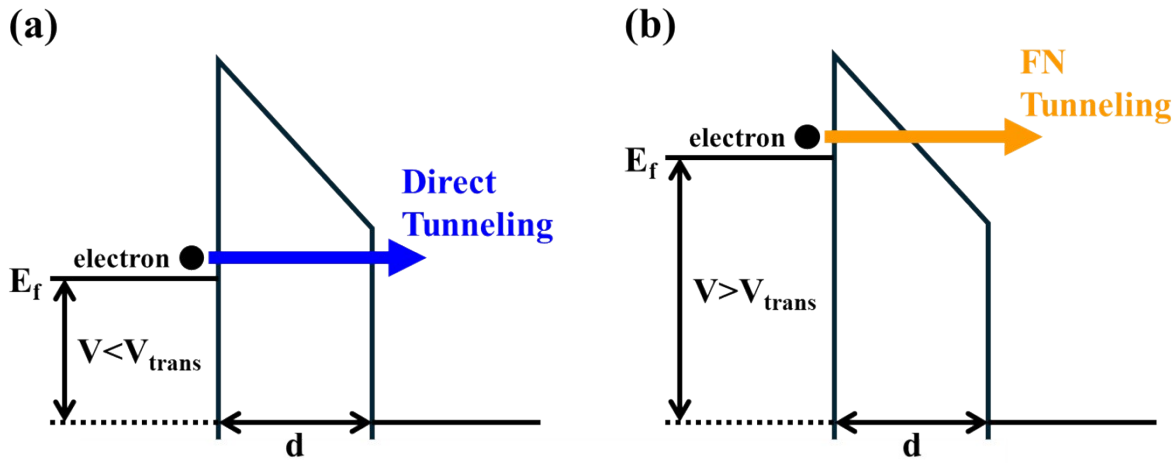

Figure S6. Schematic diagrams of (a) DT and (b) FNT.

7. Pre-spikes, post-spikes, and various net spikes applied to the ATa_2O_5 memristor to obtain Δw

The pre-synaptic spike consisted of six spikes: five spikes with a positive voltage, which gradually increased from 0.55 V to 0.75 V, and one spike with a negative voltage of – 0.65 V (Fig. S7(a)). The post-synaptic spike is the same as the pre-synaptic spike, as shown in Fig. S7(b). The net spikes applied to the ATO memristor are the difference between the pre-spike and post-spike, $[V_{pre}(t) - V_{post}(t)]$. Fig. S7(c) shows various net spikes obtained at different Δt values and applied to the ATO memristors to obtain the synaptic weight change (Δw) as a function of Δt (Fig. 7(d)). The threshold voltages (V_{th}) of the ATO memristor for potentiation and depression are approximately 1.2 V and –1.2 V, respectively, as indicated by the dotted lines in Fig. S7(c). When Δt is 40 μs (or −40 μs), the effective voltage (V_{eff}), i.e., the difference between the net spike and threshold voltage ($V_{net} - V_{th}$), is large (–0.2 V), leading to a large change in the synaptic weight of the ATO memristor. When Δt is 200 μs (or –200 μs), V_{eff} is small, leading to a small synaptic weight change, as shown in Fig. 7(d).

According to previous studies, the STDP characteristics of a biological synapse can be expressed using Eqs. (S3)[4,5]:

$$\Delta w = \begin{cases} C_+ e^{-|\Delta t|/\tau_+} + \Delta w_{0+}, & \Delta t > 0 \\ C_- e^{-|\Delta t|/\tau_-} + \Delta w_{0-}, & \Delta t < 0 \end{cases}, \quad \text{(S3)}$$

where C_+ and C_- are constants, τ_+ and τ_- are time constants, and Δw_{0+} (or Δw_{0-}) is Δw at infinite Δt (or $-\Delta t$). The STDP data for the ATO memristor, obtained from Eq. S3, fit well with the measured data, as shown in Fig. 7(d), and the C_+/C_- and τ_+/τ_- values were determined as 198.37/–197.32 and 66.90/–58.57 μs, respectively. These results confirm that the ATO memristor effectively emulates the STDP of biological synapses.

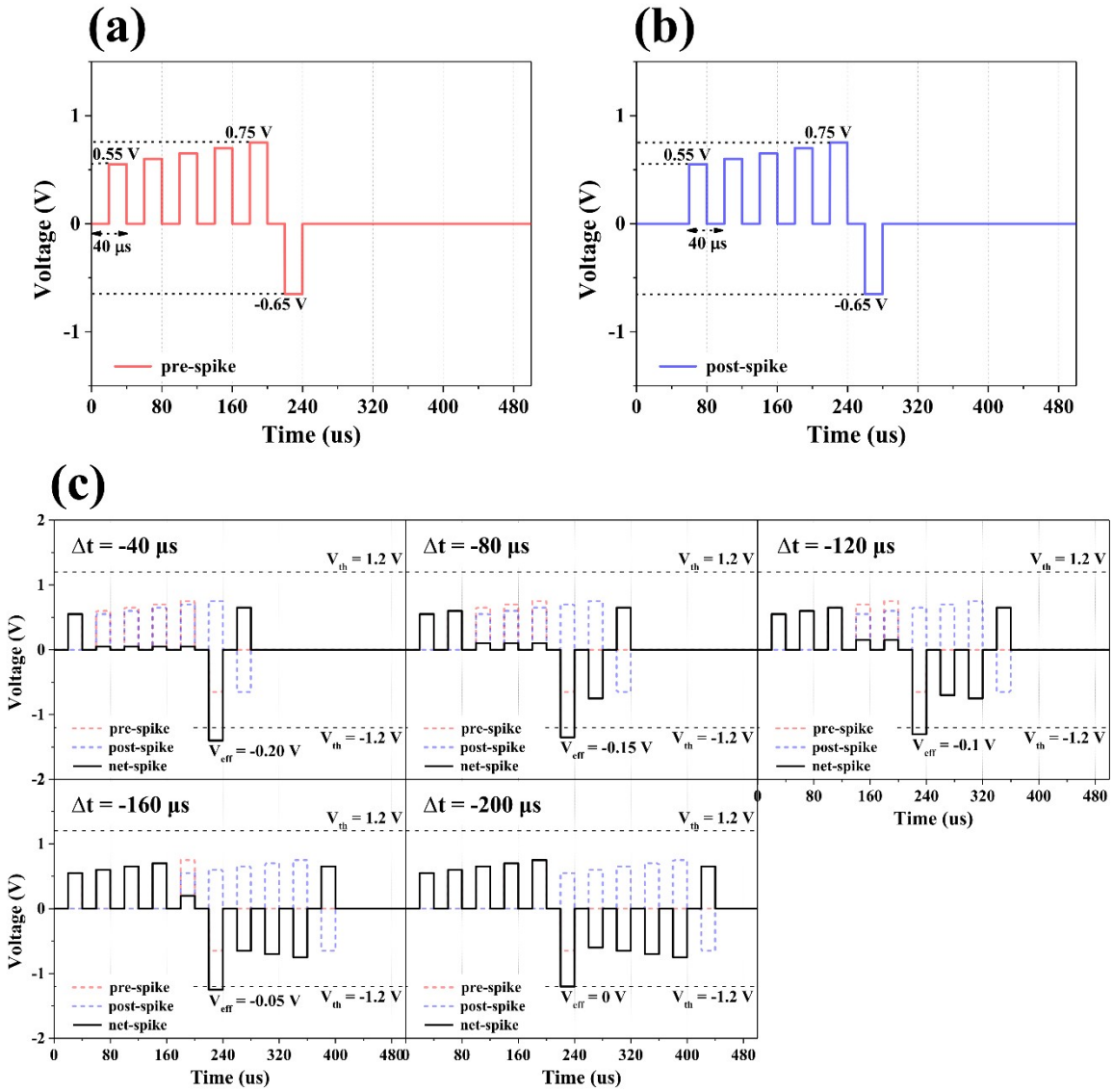

Figure S7. (a) Pre-spike, (b) post-spike, and (c) various net spikes applied to the ATa_2O_5 memristor to obtain a synaptic weight change (Δw).

References

[1] C.C. Hsu, S.Y. Wang, Y.S. Lin, Y.T. Chen, J. Alloys Compd. 779 (2019) 609–617. https://doi.org/10.1016/j.jallcom.2018.11.275.

[2] F.C. Chiu, Adv. Mater. Sci. Eng. 2014 (2014) 1–18. https://doi.org/10.1155/2014/578168.

[3] T. Ikuno, H. Okamoto, Y. Sugiyama, H. Nakano, F. Yamada, I. Kamiya, Appl. Phys. Lett. 99 (2011) 023107. https://doi.org/10.1063/1.3610486.

[4] G. Rachmuth, H.Z. Shouval, M.F. Bear, C.S. Poon, Proc. Natl Acad. Sci. U. S. A. 108 (2011) E1266–E1274. https://doi.org/10.1073/pnas.1106161108.

[5] J. Park, S.D. Jung, IEEE Trans. Circuits Syst. I. 67 (2020) 1936–1947. https://doi.org/10.1109/TCSI.2020.2966884.